Identification of endoplasmic reticulum proteins involved in glycan assembly: synthesis and characterization of P^3-(4-azidoanilido)uridine 5′-triphosphate, a membrane-topological photoaffinity probe for uridine diphosphate-sugar binding proteins

David M. RANCOUR[1] and Anant K. MENON

Department of Biochemistry, University of Wisconsin-Madison, 420 Henry Mall, Madison, WI 53706-1569, U.S.A.

Much of the enzymic machinery required for the assembly of cell surface carbohydrates is located in the endoplasmic reticulum (ER) of eukaryotic cells. Structural information on these proteins is limited and the identity of the active polypeptide(s) is generally unknown. This paper describes the synthesis and characteristics of a photoaffinity reagent that can be used to identify and analyse members of the ER glycan assembly apparatus, specifically those glycosyltransferases, nucleotide phosphatases and nucleotide–sugar transporters that recognize uridine nucleotides or UDP-sugars. The photoaffinity reagent, P^3-(4-azidoanilido)uridine 5′-triphosphate (AAUTP), was synthesized easily from commercially available precursors. AAUTP inhibited the activity of ER glycosyltransferases that utilize UDP-GlcNAc and UDP-Glc, indicating that it is recognized by UDP-sugar-binding proteins. In preliminary tests AAUTP[α-^{32}P] labelled bovine milk galactosyltransferase, a model UDP-sugar-utilizing enzyme, in a UV-light-dependent, competitive and saturable manner. When incubated with rat liver ER vesicles, AAUTP[α-^{32}P] labelled a discrete subset of ER proteins; labelling was light-dependent and metal ion-specific. Photolabelling of intact ER vesicles with AAUTP[α-^{32}P] caused selective incorporation of radioactivity into proteins with cytoplasmically disposed binding sites; UDP-Glc:glycoprotein glucosyltransferase, a lumenal protein, was labelled only when the vesicle membrane was disrupted. These data indicate that AAUTP is a membrane topological probe of catalytic sites in target proteins. Strategies for using AAUTP to identify and study novel ER proteins involved in glycan assembly are discussed.

INTRODUCTION

The enzymic machinery required for the initial assembly of the majority of cell surface carbohydrates is located in the membrane of the endoplasmic reticulum (ER) ([1,2] and references therein). This glycan-assembly apparatus consists of a wide spectrum of proteins (mainly glycosyltransferases) involved in the construction of N-glycans and glycosylphosphatidylinositol (GPI) anchors. Where information is available, these ER proteins appear to be membrane-bound (with multiple membrane-spanning domains; e.g. UDP-GlcNAc:dolichol phosphate GlcNAc phosphotransferase, [3]), highly labile, and, unlike their counterparts in the Golgi, not generally amenable to conventional protein purification [4]; with few exceptions [5–7], only partial purifications have been achieved. cDNA sequences are available in some cases through rescue of mutants by DNA transfection, but again only a few sequences are known [3,7–9]. Although genetic techniques are expected to uncover new information, other strategies must be employed in order to identify, or confirm the identity of the relevant catalytic/active polypeptides involved in glycan assembly, and to locate the catalytic site within the protein sequence and in the context of the membrane bilayer. Photoaffinity labelling techniques using radioactive, photoactive substrate analogues offer a powerful way of 'tagging' these proteins prior to conventional isolation, and avoid the necessity of using enzymic activity to monitor a protein during purification [10–13]. Purification of the tagged polypeptide then permits the acquisition of amino acid sequence, and the preparation of specific immunological reagents, all of which can be used to characterize the associated enzymic activity. Furthermore, in the case of integral membrane proteins, 'tagging' of the active site also allows for its membrane topology to be determined through protease protection experiments.

In this paper we describe a membrane-impermeant, radioactive photoaffinity reagent, P^3-(4-azidoanilido)uridine 5′-triphosphate (AAUTP[α-^{32}P]), capable of specifically labelling a broad range of ER proteins that bind uridine nucleotides/UDP-sugars. The specificity and properties of the photoprobe indicate that it would not only be capable of tagging most of the polypeptides involved in ER glycosylation but would also permit the determination of the location and membrane topology of the substrate binding site within each polypeptide. In general, AAUTP would be expected to label various glycosyltransferases (utilizing UDP-Glc, UDP-GlcNAc, and UDP-GlcA), UDP-sugar/uridine) nucleotide transporters (UDP-GlcNAc, UDP-GlcA, UDP-Xyl and a putative UDP-gal transporter [14]), and nucleoside diphosphatases. Some specific examples of potential targets include UDP-GlcNAc:phosphatidylinositol *N*-acetylglucosaminyltransferase [15,16], UDP-GlcNAc:dolichol phosphate GlcNAc phosphotransferase [3], UDP-Gal:ceramide galactosyltransferase [7], UDP-Glc:glycoprotein glucosyltransferase [17], and the UDP-Glc transporter [18].

Abbreviations used: AAUTP, P^3-(4-azidoanilido)uridine 5′-triphosphate; CA, carbonic anhydrase; ER, endoplasmic reticulum; DAPECD, 1-(3-dimethylaminopropyl)-3-ethylcarbodiimide hydrochloride; DPGS, UDP-Glc:dolichol phosphate glucosyltransferase; DPMS, GDP-Man:dolichol-phosphate mannosyltransferase; GalT, bovine milk galactosyltransferase; GlcNAcT, UDP-GlcNAc:acceptor *N*-acetylglucosaminyltransferase; GlcT, UDP-Glc:glycoprotein glucosyltransferase; GPI, glycosylphosphatidylinositol; RER, rough endoplasmic reticulum; SWER, salt-washed RER; TEA-HCl, triethanolamine hydrochloride.

[1] To whom correspondence should be addressed.

EXPERIMENTAL

Materials

Uridine 5′-[α-^{32}P]triphosphate (> 800 Ci/mmol) was purchased from Amersham (Arlington Heights, IL, U.S.A.). Uridine diphosphate *N*-acetyl-D-[6-^{3}H]glucosamine (60 Ci/mmol), uridine diphosphate [6-^{3}H]glucose (60 Ci/mmol) and guanosine diphosphate [1-^{3}H]mannose (15 Ci/mmol) were from American Radiolabeled Chemicals (St. Louis, MO, U.S.A.). 1-(3-Dimethylaminopropyl)-3-ethylcarbodiimide hydrochloride, 4-azidoaniline hydrochloride and PEI-cellulose TLC plates were purchased from Aldrich (Milwaukee, WI, U.S.A.). All nucleotides and nucleotide-sugars, phenylmethanesulphonyl fluoride, bovine milk galactosyltransferase (lactose synthase; UDP-Gal:glucose galactosyltransferase) (EC 2.4.1.22), and bovine erythrocyte carbonic anhydrase (EC 4.2.1.1) were from Sigma (St. Louis, MO, U.S.A.). Proteinase K (EC 3.4.21.14) from *Tritirachium album* was purchased from Boehringer Mannheim (Indianapolis, IN, U.S.A.). Silica TLC plates were from EM Science (Gibbstown, NJ, U.S.A.). Gel electrophoresis reagents and molecular mass markers were from Bio-Rad (Hercules, CA, U.S.A.). Other reagents and all solvents were of A.C.S. certified grade.

P^3-(4-Azidoanilido)-uridine 5′-triphosphate (AAUTP) synthesis and characterization

P^3-(4-Azidoanilido)-uridine 5′-triphosphate (Figure 1A) was synthesized according to a protocol described by Thomas and Pfeuffer [19] for synthesizing P^3-(4-azidoanilido)-guanosine 5′-triphosphate; 800 μl of 1 mM UTP in 200 mM triethanolamine hydrochloride (TEA-HCl) pH 7.2 was mixed with 800 μl of freshly prepared 50 mM 4-azidoaniline hydrochloride in 100 mM TEA-HCl, pH 7.2, and 1.6 ml 25 mM sodium hydroxide in a Reacti-vial (Pierce Chemical Co.). The reaction was started by adding 100 μl of freshly prepared 400 mM 1-(3-dimethylaminopropyl)-3-ethylcarbodiimide hydrochloride (DAPECD). After 6 h at room temperature with gentle stirring, a second aliquot (100 μl) of 400 mM DAPECD was added and the reaction mixture was incubated for a further 12 h. The reaction was stopped by extraction with water-saturated ethyl acetate to remove unreacted azidoaniline. The aqueous phase was reduced using a centrifugal vacuum concentrator (Jouan, Winchester, VA, U.S.A.) and the photoprobe was purified by preparative TLC using solvent system 1. The location of the photoprobe on the TLC plate was determined by exposing thin strips at the sides and middle of the chromatogram to 254 nm UV light. The region of silica containing the product was scraped, and the product was eluted from the silica gel with a methanol and water mixture (1:3, v/v). The extraction solvent was removed by evaporation and the product was redissolved in distilled water and stored at −20 °C. The product was quantitated by phosphate content using standard procedures (see General methods) and re-analysed by TLC to verify that only one UV-absorbing product was present before use.

Synthesis of the radiolabelled probe was performed as above but with the following modifications. One mCi of uridine 5′-[α-^{32}P]triphosphate (> 800 Ci/mmol) was dried twice from 25% methanol to remove β-sulphanylethanol used as a stabilizer by the manufacturer (note: thiol-containing compounds reduce aryl azides to aryl amines [20]) and supplemented with 20 nmol of unlabelled UTP. The volumes of the other stock solutions used were adjusted accordingly to fit the scale of the synthesis. The reaction product was located in the chromatogram by autoradiography of the TLC plate (Figure 1B), and isolated by scraping and elution. The product was quantitated based on phosphate content. Typical recovery of product was 70–75% of the UTP starting material. AAUTP[α-^{32}P] was stored as an aqueous stock solution at −70 °C and was stable until radioactive decay reduced the specific activity beyond the point of usefulness.

The unlabelled reactants and products were compared in two TLC systems (systems 1 and 2); a UV lamp (254 nm) was used to visualize the chromatograms. The R_f values obtained were: system 1 (Figure 1B): UTP (0.16), 4-azidoaniline (0.95), DAPECD+ 4-azidoaniline side product (0.72) and AAUTP (0.43); system 2: UTP (0.12), 4-azidoaniline (0.47), and AAUTP (0.37). Regions of chromatograms corresponding to azido compounds were characteristically browned/charred upon UV (254 nm) irradiation.

Phosphorus NMR spectra of UTP and AAUTP were recorded on a Bruker Avance DMX 500 spectrometer. Samples were dissolved in 50 mM Hepes/NaOH, pH 7.5 in $^{2}H_2O$. The chemical shifts (p.p.m.) were: 7.7 (α), 18.7 (β) and 4.2 (γ) for UTP and 7.6 (α), 19.3 (β) and 6.6 (γ) for AAUTP consistent with the addition of azidoaniline to the γ-phosphate. Assignments were based on Gorenstein and Shah [21].

UV-visible spectra (Figure 1C) of untreated and UV-(254 nm)-irradiated AAUTP were recorded on a Shimadzu UV-1601 UV-Visible spectrophotometer (Shimadzu, Columbus, MD, U.S.A.) with BioSpec software. The AAUTP samples (7 μM in H_2O) were analysed directly or after irradiation with UV light (254 nm, lamp intensity of 1120 μW/cm² at 7.6 cm distance, Model UVG-11, Ultra-Violet Products, San Gabriel, CA, U.S.A.) at a distance of 3 cm (to middle of sample, ±0.7 cm to ends) for 60 s. Scan time was approximately 8 s. No further decomposition was detected after 60 s of irradiation to a maximum irradiation time of 3 min (data not shown).

Preparation of vesicles from cultured cells

ER-enriched vesicles were prepared from the murine thymoma cell-line BW5147.3. Conditions for growth of the cells and details of the microsome preparation are described in Vidugiriene and Menon [15].

Preparation of rat liver rough endoplasmic reticulum (RER) vesicles and salt-washed endoplasmic vesicles (SWER)

RER vesicles were prepared from rat liver according to the method of Higgins and Fieldsend [22]. Salt-washed ER (SWER) vesicles were prepared according to Nicchitta et al. [23].

Photolabelling of bovine milk galactosyltransferase

Bovine milk galactosyltransferase (GalT) was dissolved in buffer (50 mM Hepes/NaOH, pH 7.5, 5 mM $MnCl_2$ and 5 mM $CaCl_2$) containing different amounts of AAUTP[α-^{32}P] in a total volume of 20 μl. In some experiments an equal mass amount of bovine erythrocyte carbonic anhydrase (CA) was also included in the labelling mixture. The samples were incubated at ambient temperature for 15 min followed by 1 min on ice and photolysis for the indicated times (typically 1–2 min). Photolysis was performed with a hand-held ultraviolet lamp Model UVG-11 (Ultra-Violet Products, San Gabriel, CA, U.S.A.) (254 nm, 1120 μW/cm² at 7.6 cm distance). Samples were then diluted approximately 10-fold with ice-cold 1 mM β-ME followed by trichloroacetic acid precipitation of proteins and analysis by SDS/PAGE, which was performed based on the procedure of Laemmli [24]. Autoradiography of the dried, stained gel was done at −70 °C for the indicated exposure times.

For quantitation of GalT photolabelling, reaction mixtures containing GalT (0.5 μg total protein) were photolabelled in buffer in the presence of various concentrations of AAUTP[α-^{32}P] (as above) and UDP-galactose. Parallel reactions were also performed where samples were not irradiated with UV-light. All samples were quenched with dithiothreitol (2.5 mM final concentration; 5 min at room temperature). SDS was then added (final concentration 0.08 %, w/v) and the samples were incubated for 15 min at 60 °C. Samples were then transferred to Ultrafree-MC centrifugal filter units (regenerated cellulose ultrafiltration membrane; 10000 kDa molecular mass limit) (Millipore, Bedford, MA, U.S.A.), diluted with wash buffer (50 mM Hepes/NaOH pH 7.5, 150 mM NaCl, 5 mM EDTA, and 0.03 % (w/v) SDS), and centrifuged (25 min, room temperature, 3500 ***g***). The membranes were washed three times (300 μl of wash buffer per wash, 25 min, room temperature, 3500 ***g***), then carefully excised from the filtration devices and quantitated by liquid-scintillation counting. Non-UV-irradiated sample values were used to assess the labelling background. UV-dependent incorporation of AAUTP[α-^{32}P] into protein was defined as the difference between radioactivity in samples irradiated with UV-light and those parallel samples not exposed to UV-light.

Photolabelling of microsomal proteins

The standard photolabelling reaction mixture was based on buffer conditions known to support defined enzymic activities. In general, samples were photolabelled in 250 mM sucrose, 50 mM Hepes, pH 7.5, supplemented with either EDTA, metal ions or competitors as indicated. Typical microsomal protein amounts used ranged from 25–70 μg per reaction in a total reaction volume of 50 μl. Photolabelling was performed in 1.5 ml polypropylene Eppendorf tubes with a fixed sample volume to ensure that the distance between the sample and the light source was constant. The radiolabelled photoprobe was added last to the reaction mixture with a typical final concentration of 1 μM (range used 0.05–50 μM). All reaction components were chilled on ice before mixing. Following the addition of AAUTP[α-^{32}P], samples were incubated on ice or at room temperature for 10–15 min followed by transfer to ice and photolysis for 0–2 min. Photolysis was performed with a hand-held ultraviolet lamp (Model UVG-11, as described above). Samples were diluted 5-fold with ice-cold 1 mM β-ME followed by the addition of an equal volume of cold 20 % trichloroacetic acid, and the resultant precipitated material was subsequently acetone-washed to remove lipids and prepared for SDS/PAGE. Autoradiography of the dried, stained gel was done either at -70 °C on X-ray film or on a PhosphorImager screen (Molecular Dynamics) for the indicated exposure times (typically 3–10 days).

Protease protection experiments

SWER vesicles (70 μg protein) from rat liver were suspended in photolabelling buffer containing 5 mM $MgCl_2$, 5 mM $MnCl_2$, AAUTP[α-^{32}P] (0.1–1.5 μM) either in the presence or absence of 0.5 % (w/v) NP-40. Samples were incubated at ambient temperature for 10–15 min, then transferred to ice and UV-irradiated. All samples were quenched with 1 mM β-ME (5 min, on ice), followed by proteinase K treatment (final concentration of proteinase K was 0.1 mg/ml; stock solution of 1 mg/ml in water) for 30 min on ice and quenching with 4.5 mM PMSF for 10 min on ice. Samples were diluted 4.3-fold with ice-cold water and precipitated on ice with the addition of an equal volume of 20 % (w/v) trichloroacetic acid. NP-40 (250 μg per reaction) was added after the dilution with water to act as a carrier during precipitation with trichloroacetic acid. The precipitate was collected by centrifugation, washed with acetone, and prepared for SDS/PAGE and autoradiography.

The intactness of the microsomal vesicles used was determined by assessing the resistance of UDP-Glc:glycoprotein glucosyltransferase (GlcT) to exogenously added protease. GlcT was detected by Western blotting using primary antiserum generously provided by Dr. Armando Parodi (Fundacion Campomar, Buenos Aires, Argentina) and the ECL chemiluminescence detection system (Amersham).

Assays

UDP-GlcNac:phosphatidylinositol GlcNAc transferase (GPI GlcNAcT)

The GPI GlcNAcT assay used for inhibition curves (Figure 7, below) was based on the procedure of Vidugiriene and Menon [15].

Modified conditions for the kinetic analysis of GPI GlcNAcT activity were as follows. SWER vesicles (49 μg protein) from thymoma cells in 250 mM sucrose, 50 mM Hepes/NaOH, pH 7.5, 10 mM EDTA, 0.01 % (w/v) NP-40, 0.1 mg/ml bovine liver phosphatidylinositol were incubated at 37 °C for 10 min with UDP-[^{3}H]GlcNAc (0.11–0.44 μM) in the presence (5 and 20 μM) or absence of AAUTP (total reaction volume was 50 μl). The reaction was stopped by transferring the tube to ice and the lipids were extracted by the Bligh–Dyer method [25]. Aliquots of the lower, lipid-rich organic phase were analysed by liquid-scintillation counting and TLC using system 3. Radiolabelled lipid products on thin layer chromatograms were detected using a Berthold LB 2842 automatic scanner (Berthold Analytical Instruments, Nashua, NH, U.S.A.).

Products from both assay formats were verified as authentic based on organic solubility, relative TLC mobility against standards, and, for the latter, the stimulation of product synthesis by the addition of exogenous phosphatidylinositol. The relative product mobilities in TLC system 4 were: GlcNAc-PI, 0.80, and GlcN-PI, 0.73.

UDP-Glc:dol-P glucosyltransferase (Dol-P-Glc synthase, DPGS)

The DPGS assay was based on the procedure of Vijay and Oka [26]. The total reaction volume was 50 μl. SWER vesicles from rat liver (40 μg protein) were added to a reaction mixture containing 50 mM Hepes/NaOH pH 7.5, 10 mM $MgCl_2$, 5 mM ADP, 0.05 % (w/v) NP-40, 2 μg dolichol phosphate, 1 μCi UDP-[6-^{3}H]glucose (16.7 pmol), with or without competitors, quickly mixed by vortexing, and incubated at 37 °C for 30 s (an incubation period within the linear range of activity). The reaction was terminated by adding 1 ml of ice-cold chloroform/methanol (2:1, v/v) and the lipids extracted according to Folch et al. [27]. Aliquots of the dissolved material were used for liquid-scintillation counting or TLC analysis (solvent system 4). The thin-layer chromatogram was analysed using a linear automatic scanner.

One organic-soluble radiolabelled product was synthesized with a R_f of 0.85 on TLC using solvent system 4. The amount of product was stimulated by exogenous dolichol phosphate thus supporting its identity as dolicholphosphoglucose.

UDP-Glc transporter

The assay procedure was based on that of Perez and Hirschberg [28,29]. ER vesicles were incubated with UDP[^{3}H]Glc in the presence or absence of AAUTP for 5 min at 30 °C. UDP-(^{3}H]Glc transport was determined by ultracentrifugation of the assay mixture, perchloric acid extraction of the pelleted vesicles, and scintillation counting of perchloric-acid-soluble radioactivity.

General methods

Protein was measured with the Micro BCA Protein Assay Reagent Kit (Pierce Chemical, Rockford, IL, U.S.A.). Phosphate was measured based on the procedure of Rouser et al. [30].

Thin-layer chromatography systems

Mobile phase compositions are given as volumes ratios. System 1: silica 60F_{254} or silica 60 plate; chloroform/methanol/water (10:10:3). System 2: PEI-cellulose F_{254} plate; 1 M lithium chloride. System 3: silica 60 plate; chloroform/methanol/1 M ammonium hydroxide (10:10:3). System 4: silica 60 plate; chloroform/methanol/water (10:10:2.5).

RESULTS

Synthesis and structural characterization of AAUTP

We have synthesized a radiolabelled photoactive uridine-nucleotide analogue, P^3-(4-azidoanilido)-uridine 5′-triphosphate (AAUTP[α-^{32}P], compared with UDP-glucose in Figure 1A), to use as photoaffinity reagent for the identification of UDP-sugar-binding proteins. AAUTP was purified from the reaction mixture by TLC (Figure 1B). The yield of purified material was typically 70–75 % of the input UTP (based on phosphate content). The UV-visible spectra (Figure 1C) of UV-irradiated and non-irradiated AAUTP showed a spectral shift consistent with the presence of the light-sensitive azide moiety in AAUTP. Phosphorus NMR spectra of UTP and AAUTP yielded chemical shifts consistent with the addition of azidoaniline to the γ-phosphate of UTP (see Materials and methods section).

Photolabelling of bovine milk galactosyltransferase by AAUTP[α-^{32}P]

The photolabelling properties of AAUTP were analysed using bovine milk galactosyltransferase (GalT; UDP-Gal:glucose galactosyltransferase; lactose synthase, EC 2.4.1.22). GalT is a well-characterized, commercially available soluble protein expected to bind AAUTP, e.g. [31,32].

UV-irradiation of a mixture of GalT, carbonic anhydrase (CA) (1:1.5 mol/mol) and AAUTP[α-^{32}P] resulted in the selective labelling of GalT (Figure 2A, lane 2). At higher concentrations of AAUTP[α-^{32}P] (0.25–0.5 μM), some photolabelling of CA was detectable, although the amount of labelled CA remained small ($\sim$ 2 % of the total protein-bound radioactivity at an AAUTP[α-^{32}P] concentration of 2.5 μM) and CA labelling was not saturable up to AAUTP[α-^{32}P] concentrations of 50 μM (data not shown). Neither protein was labelled in the absence of UV irradiation (Figure 2A, lane 1).

Photolabelling of GalT with AAUTP[α-^{32}P] was saturable (Figure 2B). Assuming that AAUTP[α-^{32}P] binds and labels GalT in a 1:1 molar ratio, a maximum of 25–30 % of the GalT molecules were photolabelled in the experiment shown in Figure 2B. Photolabelling of GalT was specific since AAUTP[α-^{32}P] incorporation into GalT was reduced 2-fold by including a 2-fold molar excess of UDP-Gal (10 μM) during photolabelling (Figure 2C), and eliminated altogether by including a 1000-fold molar excess of UDP-Gal (5 mM). Taken together, the data demonstrate UV light-dependent, specific and saturable labelling of a target protein by AAUTP[α-^{32}P].

Photolabelling of microsomal proteins via AAUTP[α-^{32}P] is UV-irradiation-dependent, divalent metal cation and nucleotide specific, and not dictated solely by protein abundance

The data presented above strongly suggested that AAUTP could be used for the selective photolabelling of UDP-sugar utilizing enzymes. To test this, we photolabelled rat liver ER vesicles with AAUTP[α-^{32}P]. Several protein bands were reproducibly labelled when a mixture of AAUTP[α-^{32}P] and ER vesicles (SWER) were UV-irradiated and subsequently analysed by SDS/PAGE and autoradiography (Figure 3, lanes 2–4). No labelling was seen in the absence of UV-irradiation (Figure 3, lane 1). Since different glycosyltransferases have distinct metal ion requirements, we determined the effect of divalent metal cations on the photolabelling reaction. Photolabelling was carried out in the presence of EDTA, $MgCl_2$ or $MnCl_2$ (Figure 3, lanes 2–4). The metal cations enhanced the labelling of certain proteins that were also labelled in the presence of EDTA or, interestingly, promoted the labelling of other proteins that were not detectably labelled in the presence of EDTA. Ca^{2+} was also tested and resulted

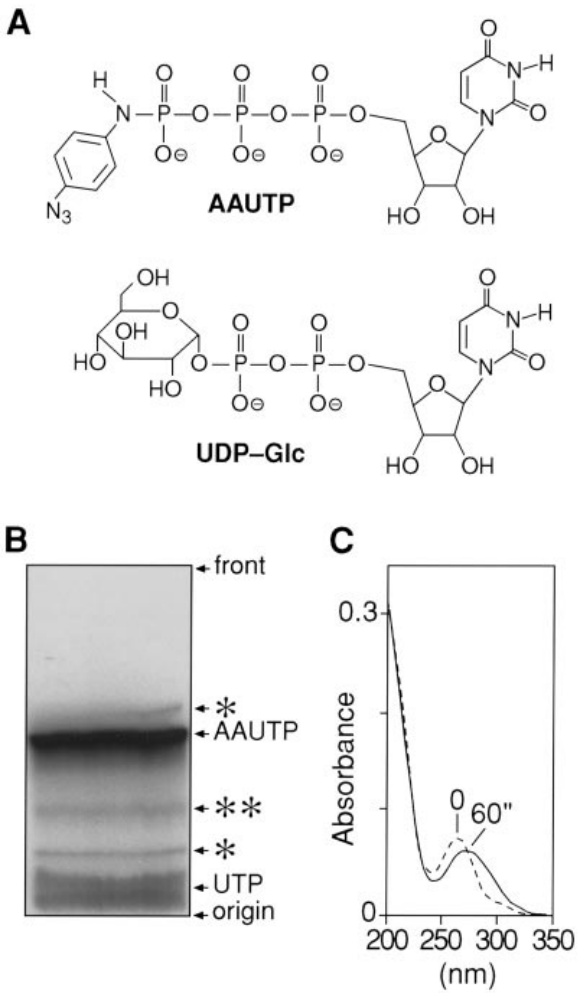

Figure 1 AAUTP: structure, purification and characterization

(**A**) Comparison of the structures of AAUTP and a representative UDP-sugar, UDP-glucose. (**B**) Autoradiogram of a thin-layer chromatogram used to purify AAUTP[α-^{32}P]. AAUTP[α-^{32}P] was synthesized and analysed as described in Materials and methods. The developed chromatogram was exposed to X-ray film for approximately 1 s. The double asterisk denotes a degradation product of AAUTP. The single asterisk denote impurities in the UTP[α-^{32}P] reactant input. (**C**) UV-visible spectra of AAUTP and UV-irradiated AAUTP. AAUTP was analysed directly (trace labelled 0, hatched line) or after exposure to 254 nm UV light for 60 s (trace labelled 60″, ——). Maxima and minima for each spectrum correspond to the following wavelengths respectively: non-UV-irradiated control: 264.5 and 241.0 nm; irradiated sample: 272.0 and 243.0 nm.

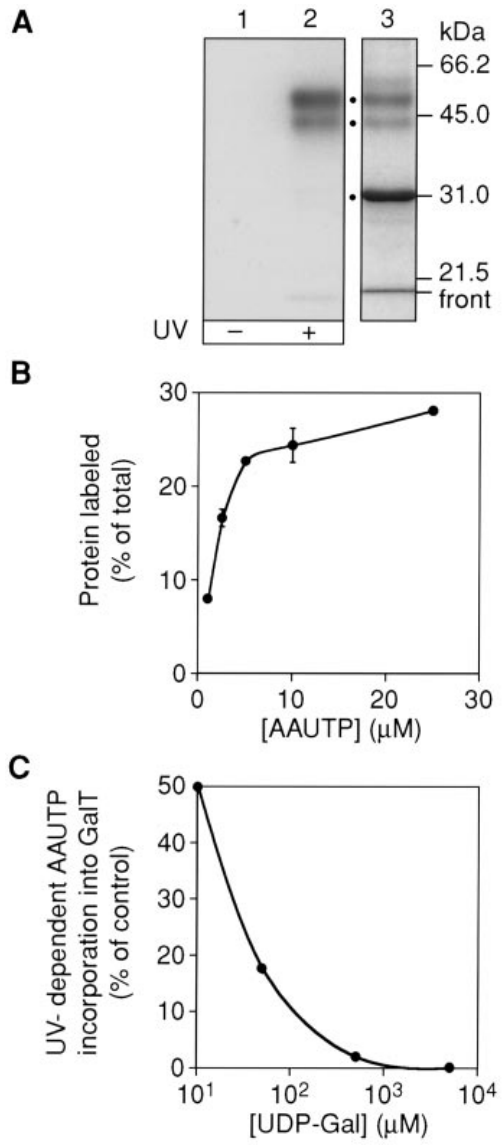

Figure 2 Photolabelling of GalT with AAUTP[α-^{32}P]

(**A**) SDS/PAGE analysis and autoradiography of an AAUTP[α-^{32}P]-photolabelled mixture of GalT and bovine erythrocyte CA. Equal mass amounts of GalT and CA (10 μg total protein per reaction) were mixed together in reaction buffer containing 0.05 μM AAUTP[α-^{32}P]. Samples (lane 2) were irradiated with UV (254 nm) light for 30 s (a control sample, lane 1, was not irradiated), trichloroacetic acid precipitated and analysed by SDS/PAGE, Coomassie staining (lane 3) and autoradiography (lanes 1, 2). The dots between lanes 2 and 3 indicate the GalT doublet (43 and 48 kDa) and CA (31 kDa). The autoradiogram was exposed to X-ray film for 4 days at -70 °C. Other bands present in the Coomassie-stained profile are impurities in the commercially obtained GalT. (**B**) Titration of AAUTP[α-^{32}P] photolabelling of GalT. Samples of GalT containing the indicated concentrations of AAUTP[α-^{32}P] were photolabelled as described in Materials and Methods. Non-UV-irradiated sample values were designated as background due to adsorption. UV-dependent incorporation of AAUTP[α-^{32}P] into protein was defined as the difference between the c.p.m. values of samples irradiated with UV-light and non-irradiated samples. The percentage protein labelled was determined by calculation of the ratio pmol of membrane-associated AAUTP[α-^{32}P] to pmol GalT (assuming an average molecular mass for GalT of 45 kDa and one uridine nucleotide binding site per molecule) in the reaction. The specific activity of the photoprobe was calculated for each experiment by liquid-scintillation counting of aliquots of stock AAUTP[α-^{32}P] solution. The values represent the average of duplicate measurements with error bars representing S.E.M. (**C**) Photolabelling of GalT by AAUTP[α-^{32}P] in the presence of a competitor, UDP-Gal. Samples of GalT in buffer containing 5 μM AAUTP[α-^{32}P] and the indicated UDP-Gal concentrations were processed and quantitated exactly as in (**B**). Numbers represent the UV-dependent incorporation of AAUTP[α-^{32}P] into membrane-associated material in the presence of UDP-Gal relative to samples which did not contain UDP-Gal. Experimental points represent single measurements.

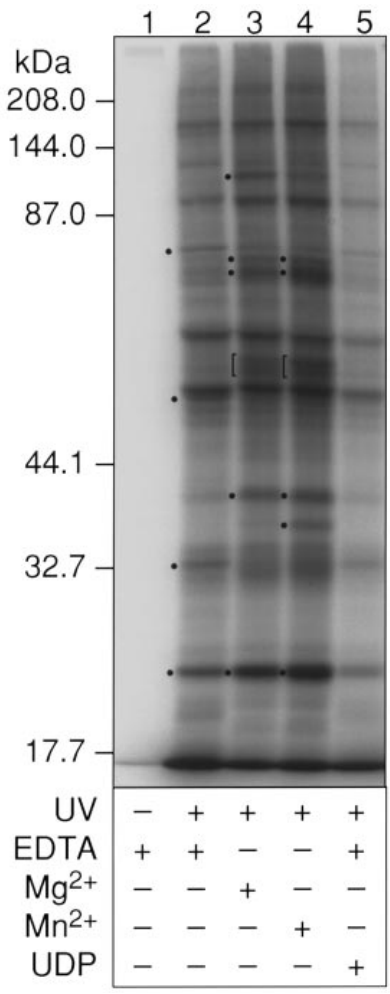

Figure 3 Photolabelling of microsomal proteins with AAUTP[α-^{32}P] is UV irradiation dependent and is affected by divalent metal cations

Rat liver RER vesicles (45 μg protein) were suspended in buffer (250 mM sucrose, 50 mM Hepes, pH 7.5, 1 μM AAUTP[α-^{32}P]) containing either EDTA (5 mM) lanes 1, 2 and 5), $MgCl_2$ (5 mM) (lane 3), or $MnCl_2$ (5 mM) (lane 4) for a final reaction volume of 50 μl. UDP (1 mM) was present in the photolabelling reaction presented in lane 5. The samples were irradiated with UV-light (254 nm) (lanes 2–4) or not (lane 1). Trichloroacetic acid precipitated material was analysed by SDS/PAGE followed by autoradiography (59 h exposure). Dots and square brackets on the autoradiogram denote examples of proteins whose photolabelling is either enhanced or dependent upon particular photolabelling conditions respectively.

in a radiolabelled protein profile most similar to that obtained in the presence of Mn^{2+} (data not shown).

As an additional test of photolabelling specificity, we labelled ER preparations with AAUTP[α-^{32}P] in the presence of various nucleoside diphosphates. A significant reduction of photolabel incorporation into protein was observed when labelling was done in the presence of UDP (Figure 3, lane 5) but not ADP, GDP or CDP (data not shown).

We next compared the SWER protein profile and its corresponding photolabelling pattern. Coomassie staining of total SWER proteins was used as a crude estimate for individual protein abundance [33]. Figure 4 shows that many of the proteins that stain heavily (examples indicated by black dots, Figure 4, lane 2) are not photolabelled, while those that are labelled correspond to proteins which either stain lightly or are not observed by Coomassie staining at all (examples indicated by

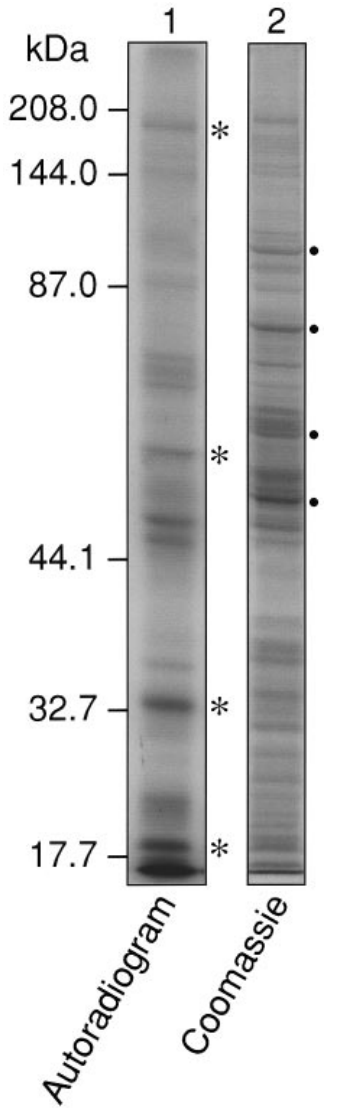

Figure 4 Specificity of photolabelling; protein abundance does not dictate labelling

Salt-washed rat liver ER vesicles (50 μg protein) were suspended in buffer (250 mM sucrose, 50 mM Hepes pH 7.5, 5 mM $MnCl_2$, 1 μM AAUTP[α-^{32}P]; final reaction volume 50 μl), photolysed, and trichloroacetic acid precipitated. Precipitated material was separated by SDS/PAGE and analysed by Coomassie staining and autoradiography (exposure time of 23 h). Asterisks denote prominent photolabelled proteins that do not have prominent corresponding Coomassie staining. Conversely, dots denote prominent stained proteins that are not photolabelled with AAUTP[α-^{32}P].

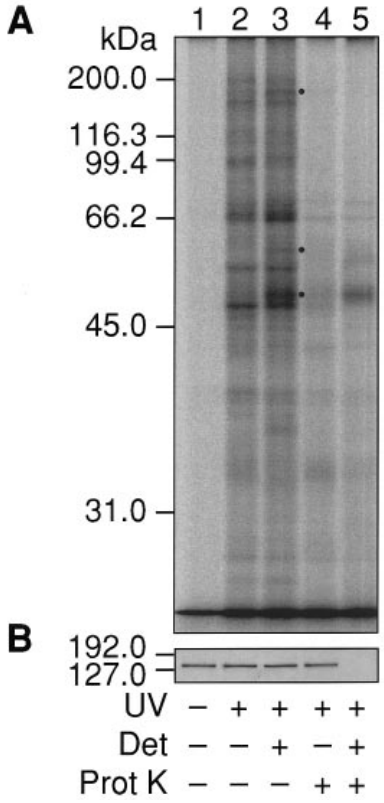

Figure 5 Photolabelling is topologically restricted in intact vesicles

(**A**) Autoradiogram of protease protection analysis of photolabelled SWER vesicles. SWER vesicles (68 μg protein per reaction) were photolabelled with 0.1 μM AAUTP[α-^{32}P] in the presence (lanes 3 and 5) or absence (lanes 1, 2 and 4) of detergent [0.5% (w/v) NP-40]. Samples (except lane 1) were irradiated with UV-light for 1 min on ice, treated with proteinase K (lanes 4 and 5) and processed as described in the Materials and methods section. Equal loading of protein equivalents per lane ($\sim$ 54 μg protein) was verified by comparison of the Coomassie staining protein profile between lanes 1–3. The autoradiogram was generated by a 10 day exposure on a Phosphorimager screen, followed by analysis with ImageQuant software (Molecular Dynamics). Dots indicate new proteins photolabelled in the presence of detergent. (**B**) Immunoblot analysis of UDP-Glc:glycoprotein glucosyltransferase (GlcT). Equal amounts of total protein ($\sim$ 6.8 μg protein) from (**A**) were resolved by SDS/PAGE, transferred to nitrocellulose, and probed with primary rabbit anti-serum against GlcT. Detection of the primary antibody was performed using a secondary anti-rabbit-HRP conjugate and the ECL system.

asterisks, Figure 4, lane 1). Thus, as seen for labelling experiments with galactosyltransferase/CA mixtures (Figure 2A), labelling of microsomal (Figure 4) proteins is not dictated by random 'sticking' of the photoprobe to abundant proteins. These data provide additional evidence of the specificity of labelling via AAUTP[α-^{32}P].

Under standard labelling conditions the photolabelled protein profile was reproducible between different experiments and independently prepared ER samples (data not shown). Some variations in the labelling profile were seen when labelling was performed with widely different concentrations of AAUTP[α-^{32}P] (compare Figure 4 with 1 μM AAUTP versus Figure 5, lane 2 with 0.1 μM AAUTP), a possible indication of the different affinities with which AAUTP binds different ER proteins. However, clear variations in the labelled protein profile were evident when RER vesicles were used versus salt-washed vesicles (Figure 3 versus Figure 4 and 5 respectively), suggesting that some peripheral membrane proteins bind AAUTP specifically.

Photolabelling of proteins via AAUTP[α-^{32}P] is topologically restricted in intact ER vesicles

In addition to using AAUTP to tag UDP-sugar/uridine-nucleotide binding proteins, the photoaffinity reagent can also be used to probe the topological orientation of sugar-nucleotide/nucleotide binding sites relative to the membrane. To do this photolabelling was carried out on sealed SWER vesicles in the presence or absence of low amounts of detergent (to disrupt the vesicle membrane barrier) and the susceptibility of the labelled material to exogenously added protease was determined. The results are shown in Figure 5.

The photolabelling of SWER proteins was UV-irradiation

dependent (Figure 5A, compare lane 1 with lanes 2 and 3). The inclusion of 0.5% (w/v) NP-40 resulted in the appearance of new labelled bands (panel A, compare lane 2 with 3; some of the new bands are denoted by dots to their right). The labelled polypeptides that migrate around 52 kDa may correspond to lumenally disposed glucuronyltransferases [34–36]. These data suggest that detergent-permeabilization of the vesicles either exposes lumenal uridine nucleotide-binding sites to the photoaffinity reagent or provides better accessibility to previously hindered cytoplasmically oriented binding sites.

Proteinase K treatment of photolabelled SWER vesicles (Figure 5A, lanes 4 and 5) diminished the intensity of the autoradiographic profile considerably both in the presence and absence of detergent. These results indicate that all the photolabelled polypeptides are susceptible to protease suggesting that photolabelling of sealed vesicles results in the exclusive labelling of cytoplasmically oriented binding sites.

To confirm that the vesicles used in the assay were sealed, we used immunoblotting to monitor the recovery of the lumenal protein UDP-Glc:glycoprotein glucosyltransferase (GlcT) after protease treatment (Figure 5B). In the absence of detergent, protease treatment of photolabelled vesicles resulted in minimal loss of GlcT (Figure 5B, lane 4), but, when detergent was added, GlcT was completely proteolysed (Figure 5B, lane 5). Based on these data, we conclude that the vesicles used were sufficiently intact so as to block access of proteinase K (28.8 kDa) to lumenal ER proteins. Thus, proteolytic elimination of AAUTP[α-^{32}P] labelled proteins in the absence of detergent (Figure 5A, lane 4 versus 2) indicates that AAUTP[α-^{32}P] cannot cross the ER membrane and binds and labels only cytoplasmically disposed binding sites in intact vesicles.

Photolabelling of GlcT

Previous photolabelling experiments indicated the presence of a photolabelled protein band migrating at approximately 150 kDa. The band could only be labelled in the presence of detergent, consistent with the proposal that it represented a lumenal uridine nucleotide or UDP-sugar-binding protein in the ER. We examined the possibility that this labelled band corresponded to GlcT, a soluble UDP-Glc-binding lumenal ER protein of molecular mass of $\sim$ 150 kDa [16]. Immunoprecipitation studies (Figure 6, lane 2) showed that this was indeed the case: a photolabelled band of $\sim$ 150 kDa was specifically precipitated by antiserum against GlcT (Figure 6, compare lanes 2 and 3). Labelling was UV-light-dependent and occurred only in (detergent) permeabilized vesicles (Figure 6, compare lanes 1 and 2), consistent with the lumenal location of GlcT [16] and the lack of membrane permeability of AAUTP (see above).

The intensity of the photolabelled GlcT band was less than previously observed for the general photolabelled SWER protein profile (Figure 4). This may be the result of inefficient immunoprecipitation. Alternatively, since GlcT acts on unfolded glycoprotein substrates [37] and the order of binding of sugar-nucleotide relative to unfolded protein substrate is not known, a seemingly low efficiency of photolabelling may be the result of limited amounts of GlcT-bound unfolded protein.

AAUTP inhibits the activity of microsomal UDP-sugar-utilizing glycosyltransferases and transporters

The data shown in Figure 6 provide one example of an ER glycosyltransferase, GlcT, that can be labelled with AAUTP[α-^{32}P]. The other labelled bands seen in typical photolabelling experiments using SWER preparations (e.g. Figure 4) are likely

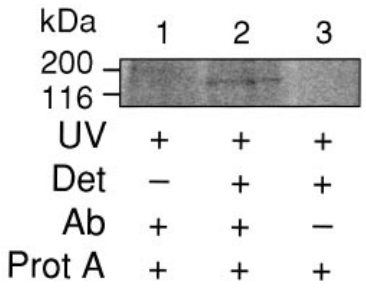

Figure 6 Immunoprecipitation of photolabelled UDP-Glc:glycoprotein glucosyltransferase

Rat liver SWER vesicles (108 μg protein per reaction) were photolabelled with 2.5 μM AAUTP[α-^{32}P] in buffer (250 mM sucrose, 50 mM Hepes/NaOH, pH 7.5, 10 mM $CaCl_2$, 5 mM $MnCl_2$) in the absence (lanes 1 and 2) or presence of detergent [0.5% (w/v) NP-40, lane 3 and 4]. Following UV irradiation (2 min on ice), all samples were quenched with β-ME and diluted 20-fold with immunoprecipitation buffer [15 mM Hepes/NaOH, pH 7.5, 150 mM NaCl, 1% (w/v) NP-40, 0.1% (w/v) SDS]. Protein-A–Sepharose (Pierce) (lanes 1–3) and primary anti-GlcT anti-serum (lanes 1 and 2) were added too the samples as indicated and allowed to mix by rotating at 4 °C overnight (15 h). Immune complexes were collected by centrifugation, washed twice with immunoprecipitation buffer and once with (15 mM Hepes/NaOH, pH 7.5, 50 mM NaCl) at room temperature. Protein samples were analysed by SDS/PAGE and autoradiography by PhosphorImager (Molecular Dynamics). The exposure time was 4 days.

to correspond to other glycosyltransferases, sugar nucleotide transporters and nucleoside diphosphates. To identify some of the ER proteins that are expected to be radiolabelled via AAUTP[α-^{32}P], we measured the ability of AAUTP to inhibit the activity of several ER glycosyltransferases and a sugar nucleotide transporter. We chose to investigate UDP-GlcNAc:phosphatidylinositol *N*-acetylglucosaminyltransferase (GPI GlcNAcT), UDP-Glc:dolicholphosphate glucosyltransferase (DPGS), and the UDP-Glc transporter.

Figure 7A provides a comparison between AAUTP and various uridine nucleotides in terms of their ability to inhibit GPI GlcNAcT activity in ER preparations from mouse thymoma cells. Unphotolysed AAUTP was similar to UTP in its ability to inhibit GPI GlcNAcT. Kinetic analysis of the reaction demonstrated that AAUTP was a competitive inhibitor of GPI GlcNAcT with an apparent K_i value of 15.4 μM AAUTP (apparent K_m for the substrate, UDP-[^{3}H]GlcNAc, was 0.57 μM). Of the three nucleotides tested, UDP was found to be the most effective at inhibiting the GlcNAcT reaction, followed by UTP and UMP. Inhibition of activity was also seen with UDP-Glc and UDP-GlcA; however, no inhibition was observed with either *N*-acetylglucosamine or *N*-acetylglucosaminyl-1-phosphate (data not shown).

Rat liver microsomal DPGS activity was also inhibited by uridine nucleotides and unphotolysed AAUTP in a concentration-dependent manner (Figure 7B). However, in this case AAUTP was a far more effective inhibitor than UTP, suggesting that the interaction between AAUTP and DPGS was not restricted to the nucleotide portion of the probe. Indeed, previous work by Kato et al. [38,39] indicates that arylphosphates are recognized by enzymes that utilize dolichol phosphate. Thus DPGS may recognize AAUTP both through its nucleotide moiety as well as its azidoarylamidophosphate extension, accounting for the potency with which AAUTP inhibits DPGS activity. In support of this proposal, preliminary experiments showed that AAUTP (but not UTP nor *p*-azidoaniline) inhibited GDP-Man:dolichol phosphate mannosyltransferase (DPMS) in a concentration-dependent manner; in this case enzymic recognition of AAUTP presumably occurred solely via the azidoarylamidophosphate moiety.

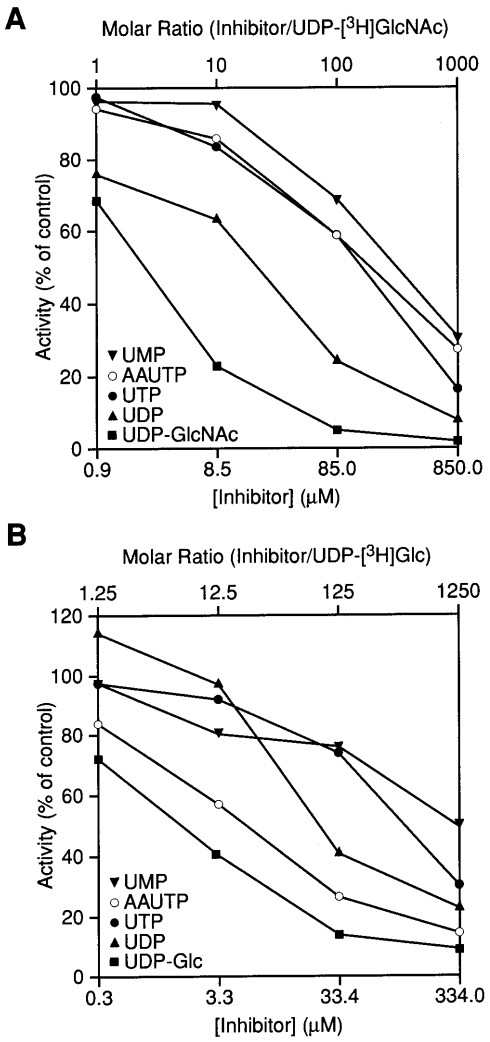

Figure 7 AAUTP and uridine nucleotides inhibit the enzymic activity of UDP-GlcNAc:phosphatidylinositol GlcNAc transferase (GlcNAcT) and DPGS

(**A**) GlcNAcT activity assayed in ER-enriched vesicles. Thymoma ER-enriched vesicles (180 μg protein) were assayed for GlcNAcT activity in the presence or absence of AAUTP and various uridine nucleotides. The concentration of the competitor used was based on the molar quantity UDP-[^{3}H]GlcNAc added to the reaction (17 pmol, 0.85 μM, $\sim$ 0.5 μCi). The activity is represented as the ratio of the amount of radioactivity incorporated into lipid in the presence of inhibitor to that of a control sample that did not contain the inhibitor. (**B**) DPGS activity assayed in SWER vesicles. SWER vesicles (40 μg protein) were suspended in reaction mixture [2 μg dolichol phosphate, 50 mM Hepes/NaOH, pH 7.5, 5 mM ADP, 10 mM $MgCl_2$, and 0.05% (w/v) NP-40] with the inclusion of inhibitors at the designated final concentrations to give a total reaction volume of 50 μl. The reaction was initiated by adding 1.0 μCi of UDP-[^{3}H]Glc (16.7 pmol; 0.33 μM) and terminated by lipid extraction and analysis (TLC system 5). The activity is represented as the ratio of the amount of radioactivity incorporated into lipid in the presence of AAUTP to that of a control experiment that did not contain the inhibitor.

We also tested the ability of AAUTP to inhibit transport of UDP-Glc into rat liver ER vesicles. Similar to the results obtained for GPI GlcNAcT (Figure 7A) our data indicate that AAUTP inhibits the time-dependent uptake of UDP-Glc into ER vesicles in a concentration-dependent manner (data not shown).

From these results we conclude that AAUTP specifically binds proteins that recognize uridine nucleotides/UDP-sugars and potentially dolichol phosphate. When applied to the ER, AAUTP is expected to be a specific photoaffinity probe for proteins that process uridine nucleotides and UDP-sugars. The single exception to this statement derives from the interaction of AAUTP with DPMS, the only known enzymic activity in the ER that utilizes dolicholphosphate but not a UDP-sugar.

DISCUSSION

In this paper we have described the synthesis and properties of a radioactive photoaffinity reagent, AAUTP[α-^{32}P], suitable for tagging UDP-sugar-binding proteins in microsomal membranes. Labelling of proteins via AAUTP[α-^{32}P] is UV-irradiation-dependent, nucleotide-specific, and saturable. Furthermore, AAUTP[α-^{32}P] is membrane impermeant and consequently can be used as a topological probe of microsomal protein UDP-sugar binding sites.

The nucleotide moiety is clearly adequate for enzymic recognition since nucleotides are able to inhibit the activity of various glycosyltransferases (e.g. GPI GlcNAcT: Figure 7A and [40]; DPGS: Figure 7B and [41,42]; UDP-GlcNAc: polypeptide GlcNAcT: [43]). In addition, nucleotides are also recognized by UDP-sugar transporters based on evidence that the transporters function as antiport systems (nucleotide-sugar in, nucleotide out; [44]) and *cis*-inhibition of activity is observed with nucleotides (UDP-GlcNAc transporter, [45]; UDP-Glc transporter, [18]; UDP-GlcA transporter, [35,46]). Nucleotide derivatives have been used to photolabel glycosyltransferases. For example, 4-thiouridine [β-^{32}P]diphosphate was used to label cytosolic O-GlcNAc transferase (UDP-GlcNAc: polypeptide GlcNAcT) [43] and 4-azido-2-nitrophenyluridylyl pyrophosphate was used to label lactose synthase [32] and β1,4-galactosyltransferase [31]. In the above cases, however, partially purified or purified enzyme sources were used in the labelling reactions.

The azidoarylamidophosphate moiety in AAUTP takes the place of the sugar moiety in UDP-sugars (Figure 1A). By eliminating the sugar moiety in the construction of a UDP-sugar-mimicking photoaffinity reagent, it could be argued that considerable binding specificity would be lost. This does not appear to be the case since AAUTP is an effective inhibitor of various UDP-sugar-utilizing glycosyltransferase activities. Inhibition of the enzymic activity of glycosyltransferases is also seen to varying degrees with either nucleotides alone or nucleotides coupled to non-substrate sugar residues but not, generally, with the sugar or sugar-1-phosphate. For example, GPI GlcNAcT that utilizes UDP-GlcNAc as substrate is inhibited by AAUTP, uridine nucleotides, UDP-Glc and UDP-GlcA, but not by GlcNAc nor GlcNAc-1-phosphate (Figure 7A, and D. M. Rancour and A. K. Menon, unpublished work). Also, in support of our nucleotide-based design hypothesis, photolabelling results with GalT show that AAUTP labels GalT in a saturable and sugar-nucleotide binding site specific fashion (Figure 2).

AAUTP labels a number of ER proteins (Figure 4, for example), roughly equivalent to the number of UDP-sugar-utilizing enzymic or transport activities known to exist in SWER vesicles. These results contrast with those obtained by others using certain UDP-sugar-based photoaffinity reagents. For example, photolabelling of microsomes with 5-azido-UDP-Glc or 5-azido-UDP-GlcA resulted in the labelling of very few bands, fewer than the known number of UDP-Glc and UDP-GlcA binding proteins [47,48]. This is surprising since the nucleotide moiety constitutes the dominant recognition motif in sugar nucleotide binding to glycosyltransferases (see above). The UDP-Glc and UDP-GlcA based photoprobes would be expected to label most UDP-sugar binding proteins, similar to AAUTP. Indeed, some cross-reactivity was observed when labelling was performed with either of the UDP-Glc or UDP-GlcA photoprobes [34,35,49], arguing for nucleotide dictated recognition. In

addition, a subset of proteins labelled by AAUTP appears to coincide with those labelled by the UDP-Glc ($\sim$ 35 kDa, Figure 4) and UDP-GlcA (52 kDa, Figure 5A, lane 3) based photoprobes ([35], and references therein). A potential explanation for the limited photolabelling observed with 5-azido-UDP-Glc or 5-azido-UDP-GlcA may be that the photoactive sugar nucleotide reagents were all derivatized at the 5-position of the uracil base. While there are clear examples where base modification is known not to inhibit binding and subsequent photolabelling of individual proteins (e.g. yeast UDP-Glc pyrophosphorylase [47], cellulose synthase from *Acetobacter xylinum* [50], and bovine UDP-GlcNAc:lysosomal-protein *N*-acetylglucosamine-1-phosphate transferase [51]), there is precedence for the base-modification to cause an adverse effect on recognition and binding by a glycosyltransferase. One example involves an α1,3-fucosyltransferase (utilizing GDP-Fuc) where 8-azido guanosine derivatives of GMP and GDP did not bind but GDP-hexanolaminyl-4-azidosalicyclic acid did [52]. The reason for this difference was concluded to be owing to azide modification of the base. Thus by modifying the nucleotide on the terminal phosphate in place of the sugar residue, as in the case of AAUTP, we eliminate the possible adverse consequences of the nucleotide base modification.

We have begun to use AAUTP to resolve a number of outstanding problems related to glycosylation reactions in the ER. These problems include (i) identification of the substrate binding component of the tetrameric protein complex required for GPI GlcNAcT activity [8,9,53–55], (ii) location of the binding site and analysis of the membrane topology of UDP-Glc:dolichol phosphate glucosyltransferase and (iii) identification of the polypeptide(s) responsible for UDP-Glc transport across the ER membrane. The latter two activities are involved in creating glucosylated N-glycans and re-glucosylating N-glycans on unfolded proteins as part of the ER calnexin/calreticulin-based quality control machinery [56]. Work on these problems is in progress.

Note added in proof (received 8 June 1998)

The phospho–amide bond in AAUTP is acid-labile. Recovery of radioactivity in AAUTP-labelled proteins is higher if non-acidic precipitants such as chloroform/methanol/water [57] are used instead of trichloracetic acid during sample work-up.

This work was supported by grant-in-aid AHA 95-GS-78 from the American Heart Association (Wisconsin Affiliate), NIH grant GM55427 and the University of Wisconsin. This study made use of services provided by the National Magnetic Resonance Facility at Madison, WI, U.S.A. which is supported by NIH grant RR02301 from the Biomedical Research Technology Program, National Center for Research Resources. Equipment in the facility was purchased with funds from the University of Wisconsin, the NSF Biological Instrumentation Program (DMB-8415048), NSF Academic Research Instrumentation Program (BIR-9214394), NIH Biomedical Research Technology Program (RR02301), NIH Shared Instrumentation Program (RR02781 and RR08438) and the U.S. Department of Agriculture. We are grateful to Dr. Armando Parodi for generously providing antiserum against UDP-Glc:glycoprotein glucosyltransferase. We thank Drs. Sebastian Bednarek, Jolanta Vidugiriene, Skip Waechter and John Rancour for advice during the course of this work, Drs. Sebastian Bednarek, Deepak Sharma and Skip Waechter for critical evaluation of early drafts of this paper, and Laura van der Ploeg and Robin Davies for producing the figures.

REFERENCES

1 Abeijon, C. and Hirschberg, C. B. (1992) Trends Biochem. Sci. **17**, 32–36
2 Lennarz, W. J. (1987) Biochemistry **26**, 7205–7210
3 Lehrman, M. A. (1991) Glycobiology **1**, 553–562
4 Elbein, A. D. and Kaushal, G. P. (1990) Methods Plant Biochem. **2**, 79–110
5 Matern, H., Bolz, R. and Matern, S. (1990) Eur. J. Biochem. **190**, 99–105
6 Shailubhai, K., Dong-Yu, B., Saxena, E. S. and Vijay, I. K. (1988) J. Biol. Chem. **263**, 15964–15972
7 Schulte, S. and Stoffel, W. (1993) Proc. Natl. Acad. Sci. U.S.A. **90**, 10265–10269
8 Takeda, J. and Kinoshita, T. (1995) Trends Biochem. Sci. **20**, 367–371
9 Inoue, N., Watanabe, R., Takeda, J. and Kinoshita, T. (1996) Biochem. Biophys. Res. Commun. **226**, 193–199
10 Haley, B. (1991) Methods Enzymol. **200**, 477–487
11 Schäfer, H.-J. (1987) in Chemical Modification of Enzymes: Active Site Studies (Eyzaguirre, J., ed.), pp. 45–62, Ellis Horwood, Chichester
12 Bayley, H. and Staros, J. V. (1984) in Azides and Nitrenes: Reactivity and Utility, (Scriven, E. F. V., ed.), pp. 433–490, Academic Press, Orlando, FL
13 Hanstein, W. G. (1979) Methods Enzymol. **56**, 653–683
14 Burger, K. N. J., van der Brijl, P. and van Meer, G. (1996) J. Cell Biol. **133**, 15–28
15 Vidugiriene, J. and Menon, A. K. (1993) J. Cell Biol. **121**, 987–996
16 Doering, T. L., Masterson, W. J., Englund, P. T. and Hart, G. W. (1989) J. Biol. Chem. **264**, 11168–11173
17 Trombetta, S. E. and Parodi, A. J. (1992) J. Biol. Chem. **267**, 9236–9240
18 Vanstapel, F. and Blanckaert, N. (1988) J. Clin. Invest. **82**, 1113–1122
19 Thomas, R. and Pfeuffer, T. (1991) Methods Enzymol. **195**, 280–286
20 Staros, J. V., Bayley, H., Standring, D. N. and Knowles, J. R. (1978) Biochem. Biophys. Res. Commun. **80**, 568–572
21 Gorenstein, D. G. and Shah, D. O. (1984) in Phosphorus-31 NMR: Principles and Applications (Gorenstein, D. G., ed.), pp. 574–575, Academic Press, Orlando, FL
22 Higgins, J. A. and Fieldsend, J. K. (1987) J. Lipid Res. **28**, 268–278
23 Nicchitta, C. V., Migliaccio, G. and Blobel, G. (1991) Cell **65**, 587–598
24 Laemmli, U. K. (1970) Nature (London) **227**, 680–685
25 Bligh, E. A. and Dyer, W. J. (1959) Can. J. Biochem. **37**, 911–917
26 Vijay, I. K. and Oka, T. (1986) Eur. J. Biochem. **154**, 57–62
27 Folch, J., Lees, M. and Stanley, G. H. S. (1957) J. Biol. Chem. **226**, 497–509
28 Perez, M. and Hirschberg, C. B. (1985) J. Biol. Chem. **260**, 4671–4678
29 Perez, M. and Hirschberg, C. B. (1986) J. Biol. Chem. **261**, 6822–6830
30 Rouser, G., Fleischer, S. and Yamamoto, A. (1970) Lipids **5**, 494–496
31 Aoki, D., Appert, H. E., Johnson, D., Wong, S. S. and Fukuda, M. N. (1990) EMBO J. **9**, 3171–3178
32 Lee, T. K., Wong, L.-J. C. and Wong, S. S. (1983) J. Biol. Chem. **258**, 13166–13171
33 Merril, C. R. (1990) Methods Enzymol. **192**, 477–488
34 Radominska, A., Berg, C., Treat, S., Little, J. M., Lester, R., Gollan, J. L. and Drake, R. R. (1994) Biochim. Biophys. Acta **1195**, 63–70
35 Radominska, A. and Drake, R. R. (1994) Methods Enzymol. **230**, 330–339
36 Tephly, T. R. and Burchell, B. (1990) Trends Pharmacol. Sci. **11**, 276–279
37 Trombetta, S. E., Bosch, M. and Parodi, A. J. (1989) Biochemistry **28**, 8108–8116
38 Kato, S., Tsuji, M., Nakanishi, Y. and Suzuki, S. (1980) J. Biochem. (Tokyo) **87**, 929–939
39 Kato, S., Tsuji, M., Nakanishi, Y. and Suzuki, S. (1981) Biochem. J. **196**, 71–79
40 Milne, K. G., Ferguson, M. A. J. and Masterson, W. J. (1992) Eur. J. Biochem. **208**, 309–314
41 Villemez, C. L. and Carlo, P. L. (1979) J. Biol. Chem. **254**, 4814–4819
42 Matern, H. and Matern, S. (1989) Biochim. Biophys. Acta **1004**, 67–72
43 Haltiwanger, R. S., Blomberg, M. A. and Hart, G. W. (1992) J. Biol. Chem. **267**, 9005–9013
44 Abeijon, C., Mandon, E. C. and Hirschberg, C. B. (1997) Trends Biochem. Sci. **22**, 203–207
45 Bossuyt, X. and Blanckaert, N. (1994) Eur. J. Biochem. **223**, 981–988
46 Bossuyt, X. and Blanckaert, N. (1993) Biochem. J. **296**, 627–632
47 Drake, R. R., Evans, R. K., Wolf, M. J. and Haley, B. E. (1989) J. Biol. Chem. **264**, 11928–11933
48 Drake, R. R., Zimniak, P., Haley, B. E., Lester, R., Elbein, A. D. and Radominska, A. (1991) J. Biol. Chem. **266**, 23257–23260
49 Drake, R. R. and Elbein, A. D. (1992) Glycobiology **2**, 279–284
50 Lin, F. C., Brown, R. M., Drake, R. R. and Haley, B. E. (1990) J. Biol. Chem. **265**, 4782–4784
51 Bao, M., Elmendorf, B. J., Booth, J. L., Drake, R. R. and Canfield, W. M. (1996) J. Biol. Chem. **271**, 31446–31451
52 Holmes, E. (1990) J. Biol. Chem. **265**, 13150–13156
53 Watanabe, R., Kinoshita, T., Masaki, R., Yamamoto, A., Takeda, J. and Inoue, N. (1996) J. Biol. Chem. **271**, 26868–26875
54 Leidich, S. and Orlean, P. (1996) J. Biol. Chem. **271**, 27829–27837
55 Watanabe, R., Inoue, N., Westfall, B., Taron, C. H., Orlean, P., Takeda, J. and Kinoshita, T. (1998) EMBO J. **17**, 877–885
56 Hammond, C. and Helenius, A. (1995) Curr. Opin. Cell Biol. **7**, 523–529
57 Wessel, D. and Flügge, U. I. (1984) Anal. Biochem. **138**, 141–143

Received 12 December 1997/8 April 1998; accepted 16 April 1998